

# The prediction of caving sequence in bord and pillar workings using Random Forest algorithm

*Depillaring of coal seams is of prime importance for coal mining industry in view of depleting superior quality coal reserve and increasing import of foreign coal. Depillaring in conjunction with caving is the most hazardous operation due to sudden roof fall. Some researchers have focused their work on roof fall risk assessment using statistical methods with a view to safety of men and machinery and to minimize accidents, down time and loss of production. Extensive research has not been done to predict roof caving sequence which is the basic requirement for successful caving operation for achieving production with zero harm potential. Roof caving is the result of interactions of all geotechnical and mining parameters including extraction area which is its main cause and contributory parameter. In this research, Random Forest, a supervised ensemble machine learning algorithm along with grid search and cross-validation is used to process the interactions among various parameters and to predict the sequential occurrence of roof caving and characterize the same as local or main fall with considerable and reliable accuracy.*

**Keywords:** Depillaring with caving, grid search, feature selection, local fall, machine learning, main fall, random forest, roof fall risk.

## 1.0 Introduction

Indian coal seams are mostly developed on bord and pillar system in which 20-30% bord-coal has been mined out. However, rest 70-80% of coal deposits are still locked in pillars (Dixit and Mishra, 2010), waiting for extraction in most of the mines, due to various geo-technical reasons. Extraction of superior quality coal locked in pillars, by depillaring is vital for Indian mining industry. The semi-mechanized depillaring with drilling and blasting for coal winning, side discharge

*Blind peer reviews carried out*

Messrs. Ram Bilash Prajapati, Rabindra Kumar Sinha and Sikandar Kumar, Department of Mining Engineering, Indian Institute of Technology (ISM), Dhanbad, Jharkhand, 826004, Dr. R.N. Gupta, Former Director of National Institute of Rock Mechanics, Bangalore, Karnataka 560070 and Ms. Divya, Mahatma Gandhi Medical College and Hospital, Jamshedpur, Jharkhand, 831012. E-mail: rbprajapati2010@gmail.com / rksinha@iitism.ac.in / sikandarbit2k11@gmail.com / guptarn1942@rediffmail.com / divya15nov@gmail.com

loader or load haul dumper for coal loading at the face and haulages for coal evacuation from face to the surface is being practiced (Singh et al. 2008). However, production, productivity and safety cannot be enhanced by this operation. (Singh et al., 2011). Support at goaf edge is provided to prevent roof falls of competent roof inside the goaf during the depillaring operation (Ghasemi et al., 2012). Roof bolt breaker line support is provided in place of conventional breaker line support (Mandal et al., 2006) in mechanized depillaring. Gupta and Prajapati (1997) have recommended use of latterly confined fully grouted roof bolts for better efficiency.

High percentage of extraction during slicing initiates roof instability which makes the active mining area almost inaccessible and difficult for manual instrumentation and monitoring in and around slicing faces (Singh, et al., 2011). Local fall takes place within twenty-four to forty-eight hours after extraction of coal and withdrawal of support in the goaf area. It does not extend up to the surface and affects only a few meters of the strata above the coal seam whereas the main fall affects the surface and takes place long after local fall. The strong and massive sandstone roof strata of Lower Gondwana age aggravates strata control problem due to the increase in void dimension caused by advancement of line of extraction. This may induce dynamic loading over surrounding pillars during caving of the strata, leading to pillar spalling and goaf edge encroachment.

Chase et al. (2002) and Mark (2010) have given guidelines for proper design of depillaring panels in deep mines including suggestions for barrier pillars to isolate active panels from nearby goaf. Mark et al. (2003) have introduced a risk factor checklist that can evaluate the overall level of roof fall risk and possible ways to reduce sudden roof fall.

Accident analysis (DGMS, 1993) reveals that depillaring in conjunction with caving is hazardous and challenging activity in coal mining due to roof fall accidents, mostly at or near the working faces which has been addressed by several researchers. Ghasemi et al.(2012) have considered 15 parameters which affect the roof fall in depillaring and developed statistical relation based on probability and consequences,  $R_{rf} = 0.33 \times [\sum_{i=1}^{15} (PF_i \times W_i)]$ , where,  $R_{rf}$  is roof

fall risk,  $PF_i$ , probability factor and  $W_i$  is weight of  $i^{\text{th}}$  parameter for risk assessment of roof fall. Maiti and Khanzode (2009) have developed model of relative risk for roof and side fall accident based on statistical analysis of potential fatalities (PF), relative risk fatality (RRF) and safety measure effectiveness (SME). (Duzgun and Einstein (2004) have used statistical methods with 1141 roof fall dataset for risk assessment using the formula, Risk = Hazard×Consequences or  $R = P [\text{Roof fall}] \times \text{Consequences}$ , where,  $R = \text{Risk of roof fall in mine}$  and  $P[\text{Roof fall}] = \text{roof fall occurrence probability in a certain period of time}$ . Consequences may involve fatalities, injuries, disabilities, equipment breakdown, downtime, etc. They compared two alternative actions “do nothing” (status quo) and “support improvement”.

Mohammadi et al. (2020), have considered nine parameters and used fuzzy integrated multi-criteria decision-making method after assigning weights and corresponding ratings for determination of cavability index (CI). Equivalent immediate roof strength (EIRS) is the thickness-weighted average of roof strata uni-axial compressive strength, given by,  $EIRS = \frac{\sum_{i=1}^n t_i \times \sigma_{ci}}{\sum_{i=1}^n t_i}$ ,  $t_i = \text{thickness of the stratum (m)}$ , = UCS of the stratum (MPa) and number of stratums in the immediate roof. And cavability index (CI),

$$CI = \sum_{i=1}^n w_i \times \frac{P_i}{P_{\max}}$$

where  $w_i$  = Weighth of the  $i^{\text{th}}$  parameter;  $P_i$  = Rate of  $i^{\text{th}}$  parameter;  $P_{\max}$  = Maximum rate of  $i^{\text{th}}$  parameter. Immediate roof has been classified on the basis of Cavability Index (5-100) in I-V categories.

Empirical formulations based on in situ measurement of strata behaviour, is very difficult due to various geotechnical and economic reasons. This is why after strata mechanics analysis of many accidents, scientists have concluded “Act of God” as the cause of accidents.

To address these issues machine learning technique, which can handle interaction of all the available parameters simultaneously has been used for analysis and prediction of systematic roof fall in depillaring districts. Random Forest, an ensemble tree-based supervised machine learning algorithm, suggested by Breiman (2001) which averages predictions over many individual random trees is applied. As the number of trees is very large, this allows for random selection of trees along with random variable selection, thus the bias is reduced and the performance is superior to other bagging algorithms and decision trees (Motwani, 2020). The algorithm is invariant to data scale, hence parameters with different units can be used directly. The algorithm is highly robust to outliers and noises in data due to its property of randomness. In this method a number of weak models are combined to form a powerful model by aggregating their “votes”. In addition, it also provides useful estimates of correlation, strength and variable importance (Breiman, 2001). Due to the aforementioned advantages, Random Forest algorithm is

preferred in various fields over other machine learning algorithms like Bagging, SVM, Decision Trees etc. It has been applied to predict rock type in drill hole (Sarantsatsral et al., 2021), coal and gas outburst disasters (Harshitha et al., 2020), detect various diseases (Jackins et al., 2021) and for selecting critical features for data classification (Chen et al., 2020).

Mathematically, it takes a training dataset as  $X = \{(x_1, y_1), (x_2, y_2), \dots, (x_n, y_n)\}$ . The classifier randomly draws a subset of samples  $(x_i, y_i)$  called bootstrap aggregation then a tree  $T_b$  is grown over the subset of samples, till the minimum node size  $n_{\min}$  is reached, by looping over the following steps:

- (i) A subset of  $m$  variables is randomly selected from a set of  $p$  variables ( $m < p$ ),
- (ii) The best split-point is picked.
- (iii) The node is split into two daughter nodes.

An ensemble of  $\{T_b\}_1^B$  trees is generated. As each tree is formed in bagging so they are identically distributed. For a classification problem,  $\widehat{C}_b(x)$  if is the class prediction of the  $b^{\text{th}}$  Random Forest tree, then the output of the tree will be  $\widehat{C}_{\text{rf}}^B(x) = \text{majority vote } \{\widehat{C}_b(x)\}_1^B$ .

## 2.0 Case study of depillaring panels in mines of Central Coalfield Ltd.

### 2.1 GEO-MINING DETAILS OF DHORIKHAS COLLIERY

DhoriKhas Colliery is located in East Bokaro coalfield in Bokaro district of Jharkhand. Dhori block lies on the main synclinal basin of East Bokaro coalfields which is covered by Talcher, Karharbari and Barakar formations of Lower Gondwana. The Barakar Formation of Lower Gondwana group occupies a major part of the minefield area. It consists of grey shale, medium to coarse grained sandstone and thick coal seams up to 61m. Exposures of Barakar rocks in this area are found in hill slopes, quarries, nallas and railway cuttings.

The mine is bounded by latitudes 23°46'00" to 23°46'53" North and longitudes 86°00'22" to 86°01'22" East. There are two units namely 4, 5 and 6 and 7 and 8 inclines, which have several seams. Karo special seam-III, is the main seam of thickness of 2.5m and gradient 1 in 6. It is being depillared by caving with diagonal line of extraction.

### 2.2 GEO-MINING DETAILS OF BHURKUNDA COLLIERY

Bhurkunda colliery lies in the Barka Sayal area of Central Coalfields Ltd. in South Karanpura coalfields in western part of Damodar valley in Ramgarh district of Jharkhand. The area forms a gently sloping ground adjoining Damodar river and is 348.5m above mean sea level (MSL). The mine lies within latitudes 23°39'00" to 23°41'00" North and longitudes 85°21'00" to 85°23'00" East. The stratigraphy and offset plan of Bhurkunda colliery are shown in Table 1 and Fig.1 respectively.

A semi-mechanized depillaring with caving having diagonal line of extraction, using universal drilling machine,

TABLE 1: STRATIGRAPHY OF THE MINE

| Name of seam | Thickness (m) | Parting (m) | Status              |
|--------------|---------------|-------------|---------------------|
| Kurse        | 2.74          |             | Exhausted           |
|              |               | 9.35        |                     |
| Upper Nakari | 3.6           |             | Exhausted           |
|              |               | 13.87       |                     |
| Lower Nakari | 1.82          |             | Exhausted           |
|              |               | 17.98       |                     |
| Upper Semana | 4.27          |             | Exhausted           |
|              |               | 19.12       |                     |
| Lower Semana | 2.84          |             | Partially extracted |
|              |               | 26.34       |                     |
| Hathidari    | 3.75          |             | Being depillared    |
|              |               | 18.54       |                     |
| Bansgarha    | 4.27          |             | Being depillared    |

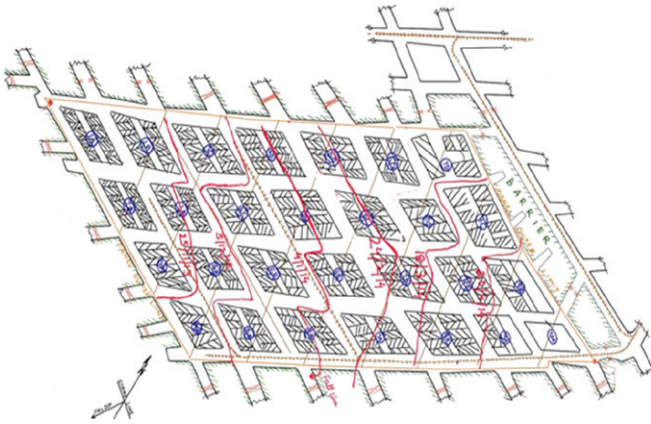


Fig.1: Bhurkunda 'B' colliery offset plan of panel-III, Hathidari seam

side discharge loader, haulages and full column grouted roof bolting system is being practiced. For strata monitoring load cell, tell tale and convergence recorder are used in both the mines.

### 2.3 DATA COLLECTION

Detailed data from both the collieries have been collected in a suitable format for application of soft computing tool. In actual model, the names of parameters have been used but for ease of depiction these parameters have been renamed as (h1-h36):

- h1 Quantity of coal in the panel (t)
- h2 Seam thickness (m)
- h3 Gradient of dip (degree)
- h4 Average thickness of cover/depth (m)
- h5 Average gallery width (m)
- h6 Pillar number
- h7 Length of pillar (m)
- h8 Width of pillar (m)
- h9 Length of depillaring panel (m)
- h10 Width of depillaring panel (m)

- h11 Sandstone percentage (%)
- h12 Coal left in immediate roof (m)
- h13 Coal layer thickness value (LTV) (cm)
- h14 Coal SFI value
- h15 Coal slack durability index (SDI, %)
- h16 Coal UCS (kg/cm<sup>2</sup>)
- h17 Coal GWS value (mL/min)
- h18 Total rating of coal
- h19 Thickness of immediate rock (m)
- h20 Rock LTV (cm)
- h21 Rock SFI
- h22 Rock SDI (%)
- h23 Rock UCS (kg/cm<sup>2</sup>)
- h24 Rock GWS value (mL/min)
- h25 Total rating of rock
- h26 Combined rock mass rating (RMR)
- h27 Rock load (t/m<sup>2</sup>)
- h28 Tensile strength (kg/cm<sup>2</sup>)
- h29 Poisson's ratio
- h30 Young's modulus (GPa)
- h31 Area of fall (m<sup>2</sup>)
- h32 Days
- h33 Rock type shale (S)
- h34 Rock type shaly sandstone (SH SST)
- h35 Rock type sandstone (SST)
- h36 Fall (Model 1 – No fall (0) or Fall (1),

Model 2 – Local fall (0) or Main fall (1)).

where, UCS - Uni-axial compressive strength.

SFI - Structural feature Indices

GWS - Groundwater seepage

### 3.0 Proposed methodology

In the current research, two different models are prepared, to predict the occurrence of a caving sequence in underground coal mine (Model 1) and another to differentiate between local and main fall (Model 2). The input parameters are chosen after extensive literature review and relevant data is collected.

During the data-preprocessing phase data has been cleaned and any missing values identified have been dropped. The categorical variables are converted to dummy variables. The data is then ready to be fed into the classifier. Approximately, 30% of the data has been kept aside for testing the model.

Two random forest classifier models are built (Fig.2), after hyperparameter tuning by grid search and fit on its respective training dataset and cross-validated. Then, the models have been tested on their respective test data.

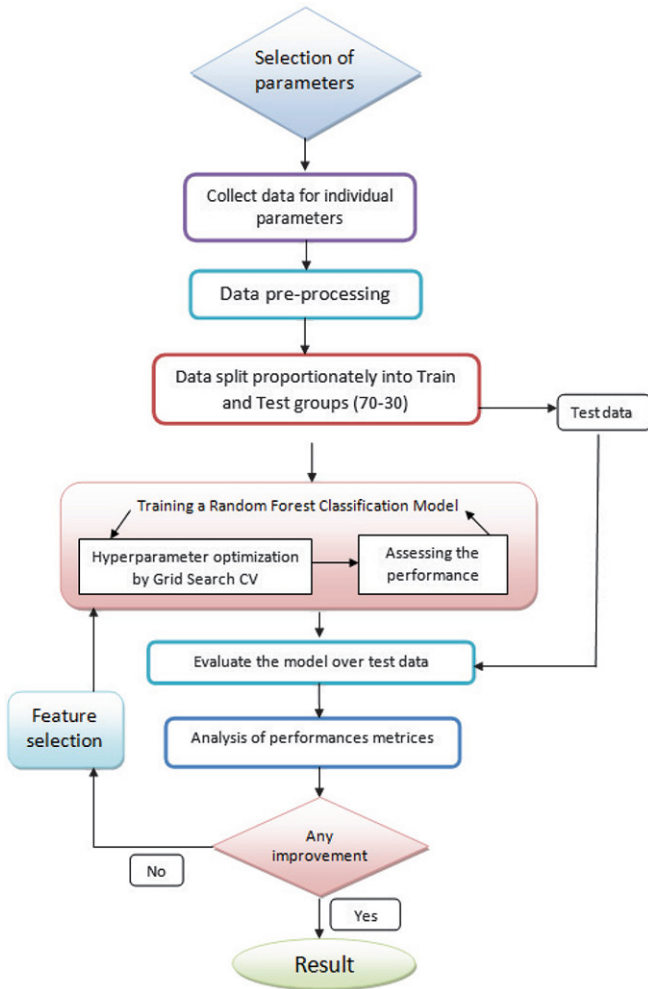


Fig.2 The procedure of model creation

### 3.1 PARAMETERS AND DATASET OF MODELS

Brief overview of correlation among parameters can be visualized from scatter plots (Fig.3,4,5) and pearson correlation plot (Fig.6). The dataset for prediction of occurrence of “Fall” (Model 1), has 323 data of which 118 data of “No fall (0)” and 205 data of “Fall (1)”. The dataset for prediction of occurrence of either local or main fall (Model 2), has 207 data, containing 120 data of “Local fall (0)” and 87 data of “Main Fall (1)” (Table 2).

### 3.2 TRAINING OF MODEL

The data is split in the ratio of 70:30 for training and testing. 5-fold cross validation has been performed during the process. As there are several hyperparameters in a Random Forest model which can be tweaked to enhance the overall accuracy. This necessitates the use of grid search for hyperparameter selection (Table 3) this has been kept same for both the models during the whole training process, the chosen set is given in Table 4.

The importance of different parameters used during training of models are analyzed. The feature importance bar

plot of model 1 (No fall (0) or fall (1)) (Fig.7) shows that the classifier gives importance to area, h31(0.414), days, h32 (0.277), pillar number, h6(0.022), SDI, h15(0.006).

The feature importance bar plot of model 2 (Fig.8) (local fall (0) or main fall (1)) shows that the classifier gives importance to area (0.409), days (0.154), tensile strength (0.037), rock UCS value (0.037).

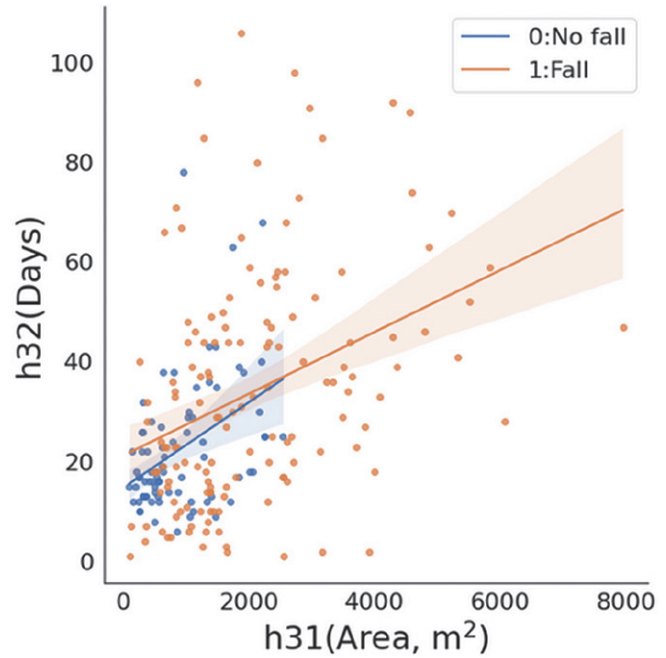


Fig.3: The plot between area and days shows that a fall of larger area, takes a longer time to occur

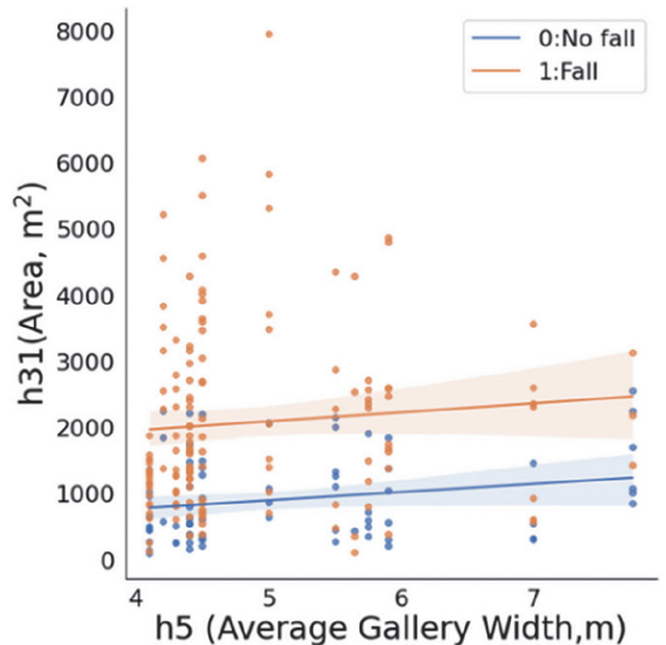


Fig.4: The plot depicts that as the average gallery width increases, falls of a larger area usually occurs

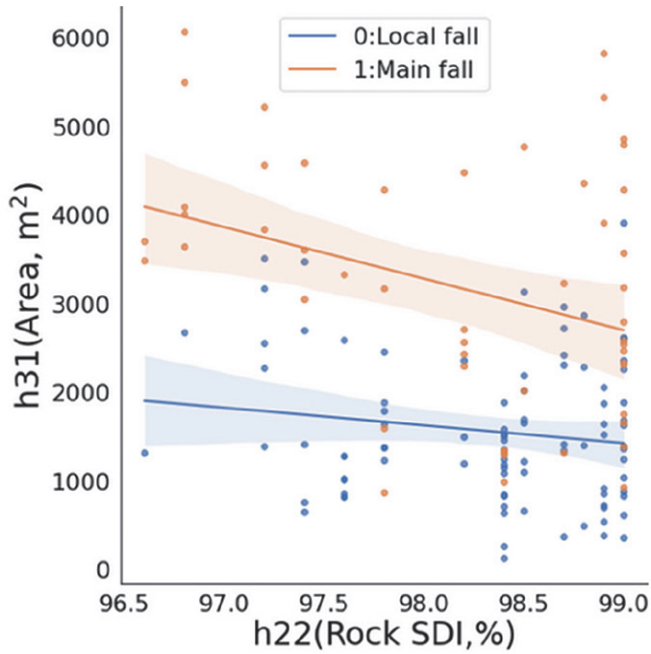


Fig.5: The plot depicts that as the rock SDI increases, the area of fall decreases as high SDI weakens the rock

After analyzing the feature importance plots of the two models, an attempt is made to understand the complex interplay of these features and their effect on model performance. For this, the last eight least important features have been dropped out from training and test dataset of both the models then grid search and cross-validation with same specifications is run. The performance of the resulting models is analyzed and compared to the corresponding previous models.

The set of optimum hyperparameters obtained after removing the last eight least important features of corresponding models. (Table 5)

The feature importance after removing the last eight least important features (coal SFI; h14, coal GWS; h17, rock GWS; h24, rocktype S; h33, SH-SST; h34, SST; h35, coal left in roof; h12, coal UCS; h16) of model 1 (fall (0) or no fall (1)) is given in (Fig.9)

Feature importance after removing the last eight least important features (coal SFI; h14, coal GWS; h17, rock GWS; h24, rocktype S; h33, SH-SST; h34, SST; h35, coal left in roof; h12, sandstone %; h11) of model 2 (local fall (0)/main fall (1)) is given in Fig.10.

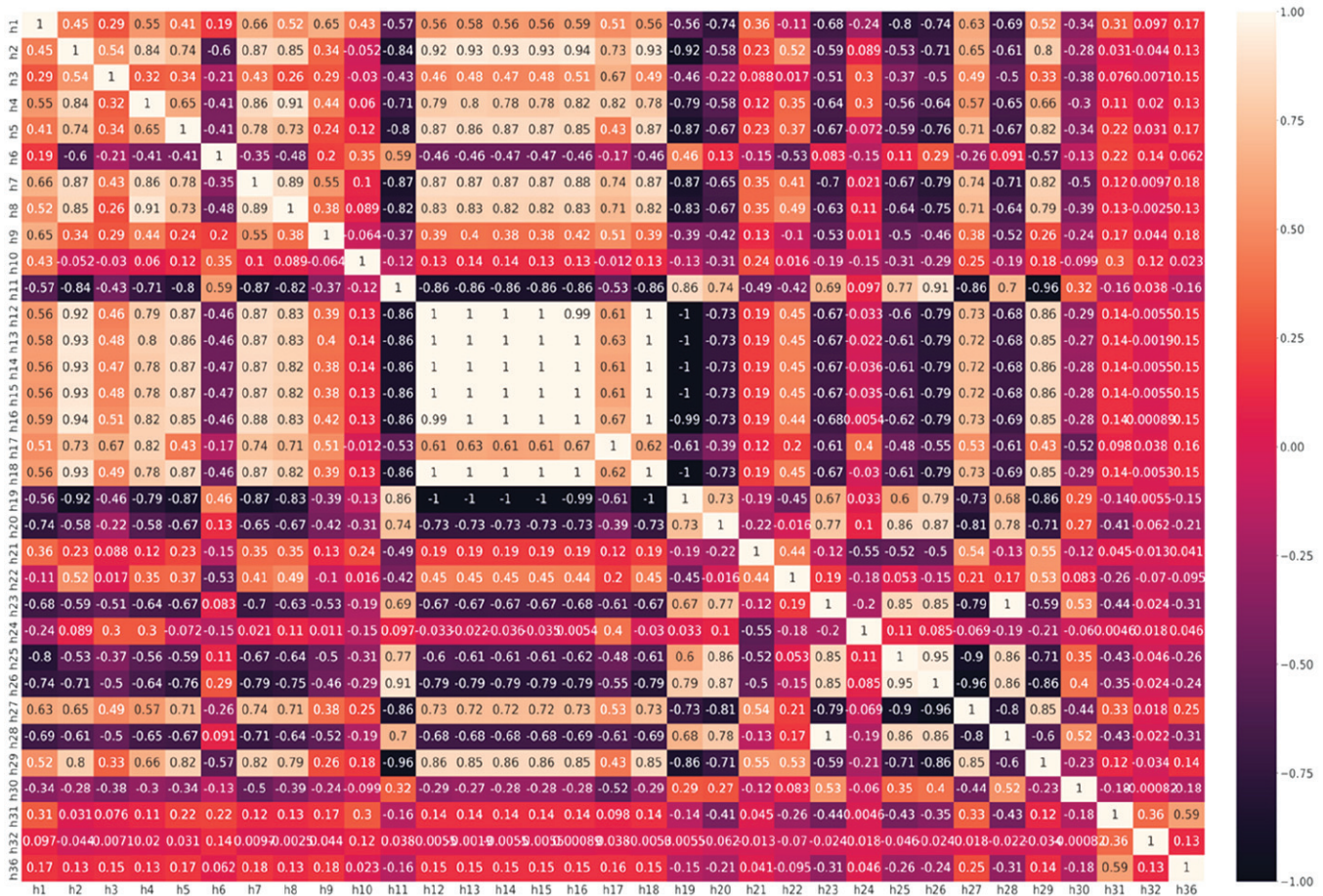


Fig.6: The Pearson correlation plot shows that occurrence of local and main fall is highly correlated with area, h31(0.59), length of pillar, h7(0.18) and negatively correlated with tensile strength, h28(-0.31) and sandstone %, h11(-0.16)

TABLE 2: OVERVIEW OF TRAINING DATASET FED TO MODEL 2

|       | h1       | h2     | h3     | h4     | h5     | h6     | h7     | h8     | h9     | h10    | h11    | h12    | h13    | h14    | h15    | h16    |
|-------|----------|--------|--------|--------|--------|--------|--------|--------|--------|--------|--------|--------|--------|--------|--------|--------|
| count | 142.00   | 142.00 | 142.00 | 142.00 | 142.00 | 142.00 | 142.00 | 142.00 | 142.00 | 142.00 | 142.00 | 142.00 | 142.00 | 142.00 | 142.00 | 142.00 |
| mean  | 55074.20 | 3.22   | 0.17   | 82.38  | 4.85   | 57.73  | 24.95  | 21.22  | 243.01 | 131.77 | 78.88  | 0.22   | 1.25   | 1.97   | 27.82  | 77.25  |
| std   | 26514.84 | 0.55   | 0.12   | 62.90  | 0.88   | 22.20  | 5.01   | 4.82   | 65.93  | 38.30  | 17.37  | 0.35   | 2.01   | 3.16   | 44.58  | 124.32 |
| min   | 3400.00  | 2.70   | 0.12   | 27.50  | 4.10   | 28.00  | 20.00  | 16.00  | 130.00 | 76.00  | 55.00  | 0.00   | 0.00   | 0.00   | 0.00   | 0.00   |
| 25%   | 38400.00 | 2.80   | 0.14   | 49.50  | 4.30   | 40.00  | 20.00  | 18.00  | 177.50 | 115.00 | 55.00  | 0.00   | 0.00   | 0.00   | 0.00   | 0.00   |
| 50%   | 57000.00 | 3.00   | 0.15   | 58.00  | 4.40   | 49.50  | 24.00  | 20.00  | 250.00 | 125.00 | 82.80  | 0.00   | 0.00   | 0.00   | 0.00   | 0.00   |
| 75%   | 70000.00 | 3.75   | 0.17   | 99.99  | 5.50   | 85.00  | 28.00  | 24.42  | 300.00 | 150.00 | 94.00  | 0.75   | 4.20   | 7.00   | 98.02  | 246.40 |
| max   | 96000.00 | 4.27   | 0.67   | 277.03 | 7.75   | 98.00  | 36.62  | 34.75  | 345.00 | 250.00 | 94.00  | 0.80   | 4.60   | 7.00   | 99.60  | 295.40 |

|       | h17    | h18    | h19    | h20    | h21    | h22    | h23    | h24    | h25    | h26    | h27    | h28    | h29    | h30    | h31     | h32    | h36    |
|-------|--------|--------|--------|--------|--------|--------|--------|--------|--------|--------|--------|--------|--------|--------|---------|--------|--------|
| count | 142.00 | 142.00 | 142.00 | 142.00 | 142.00 | 142.00 | 142.00 | 142.00 | 142.00 | 142.00 | 142.00 | 142.00 | 142.00 | 142.00 | 142.00  | 142.00 | 142.00 |
| mean  | 0.13   | 15.99  | 1.78   | 13.71  | 6.50   | 98.28  | 698.38 | 0.48   | 70.17  | 60.10  | 2.30   | 69.60  | 0.14   | 5.11   | 2137.21 | 34.20  | 0.36   |
| std   | 0.33   | 25.62  | 0.35   | 4.51   | 1.62   | 0.70   | 201.11 | 0.50   | 5.69   | 9.01   | 1.35   | 20.31  | 0.07   | 0.56   | 1314.97 | 23.31  | 0.48   |
| min   | 0.00   | 0.00   | 1.20   | 5.10   | 5.00   | 96.60  | 322.70 | 0.00   | 55.40  | 40.40  | 0.82   | 32.27  | 0.06   | 4.22   | 130.00  | 1.00   | 0.00   |
| 25%   | 0.00   | 0.00   | 1.25   | 10.25  | 5.00   | 97.80  | 526.35 | 0.00   | 64.30  | 50.10  | 1.43   | 52.64  | 0.08   | 4.60   | 1220.75 | 16.25  | 0.00   |
| 50%   | 0.00   | 0.00   | 2.00   | 14.00  | 7.00   | 98.40  | 780.50 | 0.00   | 72.30  | 65.07  | 1.57   | 78.05  | 0.10   | 5.22   | 1689.50 | 29.50  | 0.00   |
| 75%   | 0.00   | 55.80  | 2.00   | 18.40  | 7.00   | 98.90  | 864.22 | 1.00   | 73.28  | 65.95  | 3.40   | 86.42  | 0.21   | 5.40   | 2780.00 | 47.75  | 1.00   |
| max   | 1.00   | 58.50  | 2.00   | 20.00  | 13.00  | 99.00  | 984.40 | 1.00   | 79.82  | 71.83  | 6.10   | 98.44  | 0.28   | 7.04   | 6068.00 | 106.00 | 1.00   |

TABLE 3: HYPERPARAMETER SPACE

| Hyperparameters  | Grid values      |
|------------------|------------------|
| n-estimators     | 200, 500, 700    |
| Maximum features | auto, sqrt, log2 |
| Maximum depth    | 15, 18, 20       |
| Min sample split | 2,5              |
| Min sample leaf  | 1,2              |
| Criterion        | gini, entropy    |

TABLE 4: THE OPTIMAL GRID VALUES

| Hyperparameters  | Model 1 (no fall (0)/fall (1)) | Model 2 (local fall (0)/ main fall (1)) |
|------------------|--------------------------------|---|
| n-estimators     | 200                            | 700                                     |
| Maximum features | sqrt                           | Sqrt                                    |
| Maximum depth    | 20                             | 20                                      |
| Min sample split | 5                              | 5                                       |
| Min sample leaf  | 1                              | 2                                       |
| Criterion        | entropy                        | gini                                    |

### 3.3 RESULT AND ANALYSIS

3.3.1 Training score: The score of the models when tested over the training dataset itself is enlisted in Table 6.

From, the training score it is evident that for Model 1, there is a decline of (-0.0045), whereas in case of Model 2 there is an increase in training score by +0.0071.

### 3.4 CONFUSION MATRIX

The confusion matrix represents the following information (Table 7):

This helps in calculating the accuracy, precision, recall, true positive rate and false positive rate and f1 score of the model created which together depicts the generalization

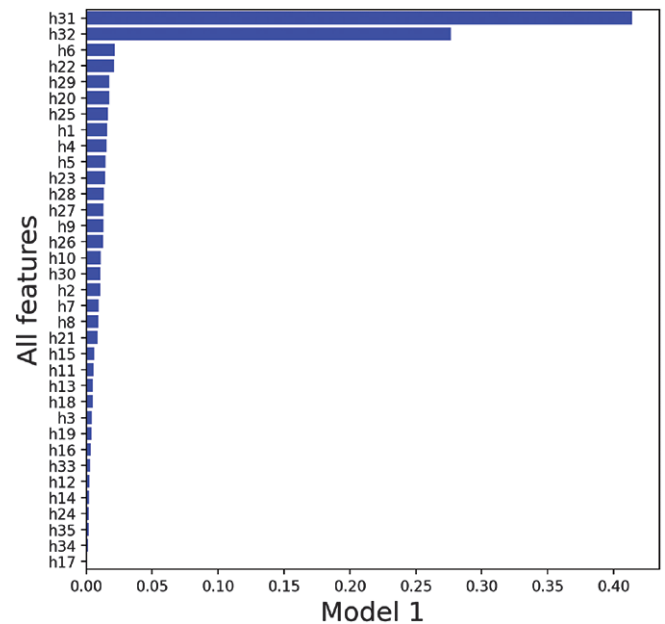


Fig.7: Feature importance of Model 1 (fall or no fall)

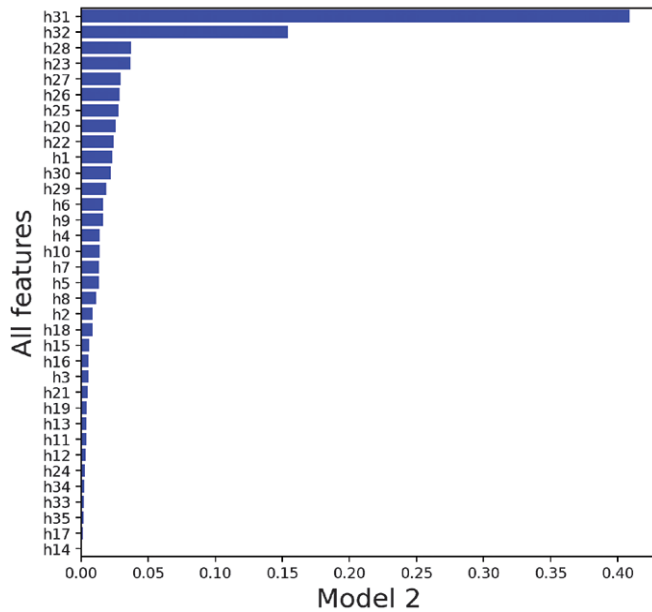


Fig.8: Feature importance of Model 2 (local or main fall)

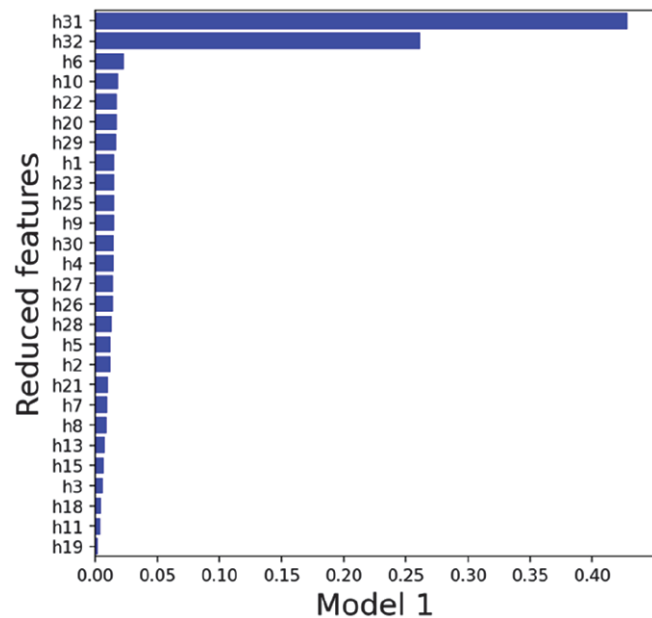


Fig.9: Feature importance of Model 1 (reduced features)

capability of the model and aids in evaluation of the model (Goutte and Gaussier, 2005). The matrices obtained from the aforementioned models is given in Table 8, which shows that Model 1 with all features as well as reduced features, can correctly classify 27 out of 41 cases of “no fall” and correctly identifies 54 out of 62 cases of “fall”. Model 2 with all the features correctly identifies 27 cases out of 28 cases of “local fall” and misclassifies 1 case as main fall whereas it correctly identifies 26 cases of main fall out of 36 cases of the category and incorrectly identifies 10 such cases as local fall. However, the impact of feature selection is evident from the results obtained from model 2 with reduced features in which the

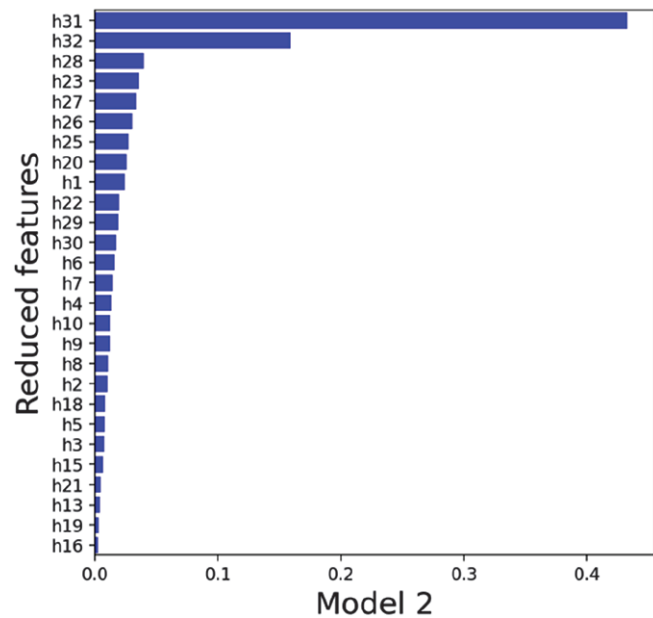


Fig.10: Feature importance of Model 2 (reduced features)

TABLE 5: OPTIMAL SET AFTER FEATURE REDUCTION

| Hyperparameters  | Model 1 (no fall (0)/fall (1)) | Model 2 (local fall (0)/main fall (1)) |
|------------------|--------------------------------|--|
| n-estimators     | 200                            | 200                                    |
| Max features     | sqrt                           | auto                                   |
| Max depth        | 20                             | 15                                     |
| Min sample split | 2                              | 2                                      |
| Min sample leaf  | 2                              | 2                                      |
| Criterion        | entropy                        | gini                                   |

TABLE 6: TRAINING SCORE

| Training score | With all features | With reduced features |
|----------------|-------------------|-----------------------|
| Model 1        | 0.9272            | 0.9227                |
| Model 2        | 0.8943            | 0.9014                |

TABLE 7: CONFUSION MATRIX

| Predicted class | True class no fall  | True class fall     |
|-----------------|---------------------|---------------------|
| fall no fall    | True positive (TP)  | false positive (FP) |
| fall fall       | False negative (FN) | true negative (TN)  |

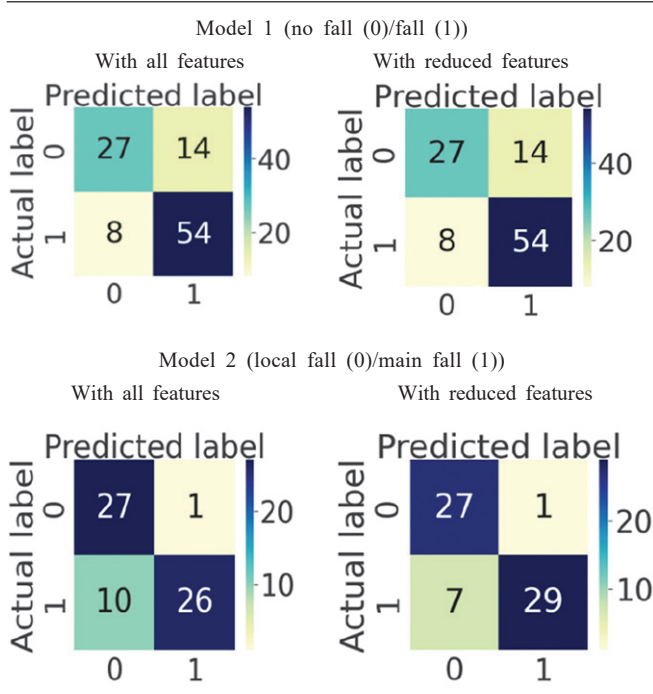
ability of the model to correctly predict the occurrence of main fall increases to 29 cases out of 36 cases.

### 3.5 CLASSIFICATION REPORT

The classification report of the models is given in Table 9. Highest accuracy of 79% is achieved over test dataset for predicting the occurrence of fall (Model 1 with all features) and highest accuracy of 88% over test data for predicting the occurrence of local or main fall.

The predictive accuracy after removing eight least important features remains almost in case of Model 1, whereas

TABLE 8 CONFUSION MATRIX OF THE MODELS



the accuracy of prediction of local and main fall gets enhanced by +5% in case of Model 2, those features may have been declining the model performance.

3.6 ROC CURVE

The ROC curve is formed by plotting the true positive rate (sensitivity) on y-axis and the false positive rate on x-axis which is in turn calculated from the confusion matrix as:

$$\text{True positive rate} = \frac{TP}{TP + FN}$$

$$\text{False positive rate} = 1 - \text{true negative rate}$$

$$1 - \frac{TN}{TN + FP}$$

(True negative rate is also known as specificity.) The curves formed after testing the models over test dataset has been shown in Fig.11. These curves act as simple but effective tool for assessing the model performance, which can be summarized as the larger the area under the curve (AUC) (Table 10) the better is the classification ability of the model (Bradley, 1997).

4.0 Conclusions

The data collected from two collieries has been employed to create models which predict the occurrence of fall and classify it as local and main fall with substantial and reliable accuracy. For field implementation of the model, the different anticipated extraction areas along with other parameters are tested by the models for prediction of fall and to classify the same as local or main fall. The set of such areas which passes the tests gives the sequence of local and main fall and act as an

TABLE 9: CLASSIFICATION REPORT

| Model 1 (No fall (0)/ Fall (1))         |           |        |          |         |
|---|-----------|--------|----------|---------|
| With all features                       |           |        |          |         |
|   | Precision | Recall | f1-score | Support |
| 0                                       | 0.77      | 0.66   | 0.71     | 31      |
| 1                                       | 0.79      | 0.87   | 0.83     | 64      |
| Accuracy                                |           |        | 0.79     | 103     |
| Macro avg                               | 0.78      | 0.76   | 0.77     | 103     |
| weighted avg                            | 0.79      | 0.79   | 0.79     | 103     |
| With reduced features                   |           |        |          |         |
|   | Precision | Recall | f1-score | Support |
| 0                                       | 0.76      | 0.63   | 0.69     | 11      |
| 1                                       | 0.78      | 0.87   | 0.82     | 62      |
| Accuracy                                |           |        | 0.78     | 103     |
| Macro avg                               | 0.77      | 0.75   | 0.76     | 103     |
| weighted avg                            | 0.78      | 0.78   | 0.77     | 103     |
| Model 2 (Local fall (0)/ Main fall (1)) |           |        |          |         |
| With all features                       |           |        |          |         |
|   | Precision | Recall | f1-score | Support |
| 0                                       | 0.73      | 0.96   | 0.83     | 28      |
| 1                                       | 0.96      | 0.72   | 0.83     | 36      |
| Accuracy                                |           |        | 0.83     | 64      |
| Macro avg                               | 0.85      | 0.84   | 0.83     | 64      |
| weighted avg                            | 0.86      | 0.83   | 0.83     | 64      |
| With reduced features                   |           |        |          |         |
|   | Precision | Recall | f1-score | Support |
| 0                                       | 0.79      | 0.96   | 0.87     | 28      |
| 1                                       | 0.97      | 0.81   | 0.88     | 36      |
| Accuracy                                |           |        | 0.88     | 64      |
| Macro avg                               | 0.88      | 0.88   | 0.87     | 64      |
| weighted avg                            | 0.89      | 0.88   | 0.88     | 64      |

TABLE 10: COMPARISON OF AUC OF MODELS

|  | With all features | With reduced features |
|--|-------------------|-----------------------|
| Model 1 (no fall (0)/fall (1))         | 0.765             | 0.753                 |
| Model 2 (local fall (0)/main fall (1)) | 0.843             | 0.885                 |

indicator for taking advance precautions for safety of workers and equipment in the caving panel against fall. It can be inferred that the quality of data and features selected for creating the model plays a crucial role in efficacy of the model, as is evident from the result of this research that if the parameters are selected on the basis of their importance an increase in accuracy of model's result is observed.

Acknowledgement

The authors are grateful to the management of Central Coalfield Ltd. For extending their support with the necessary information and data required for this study. The views

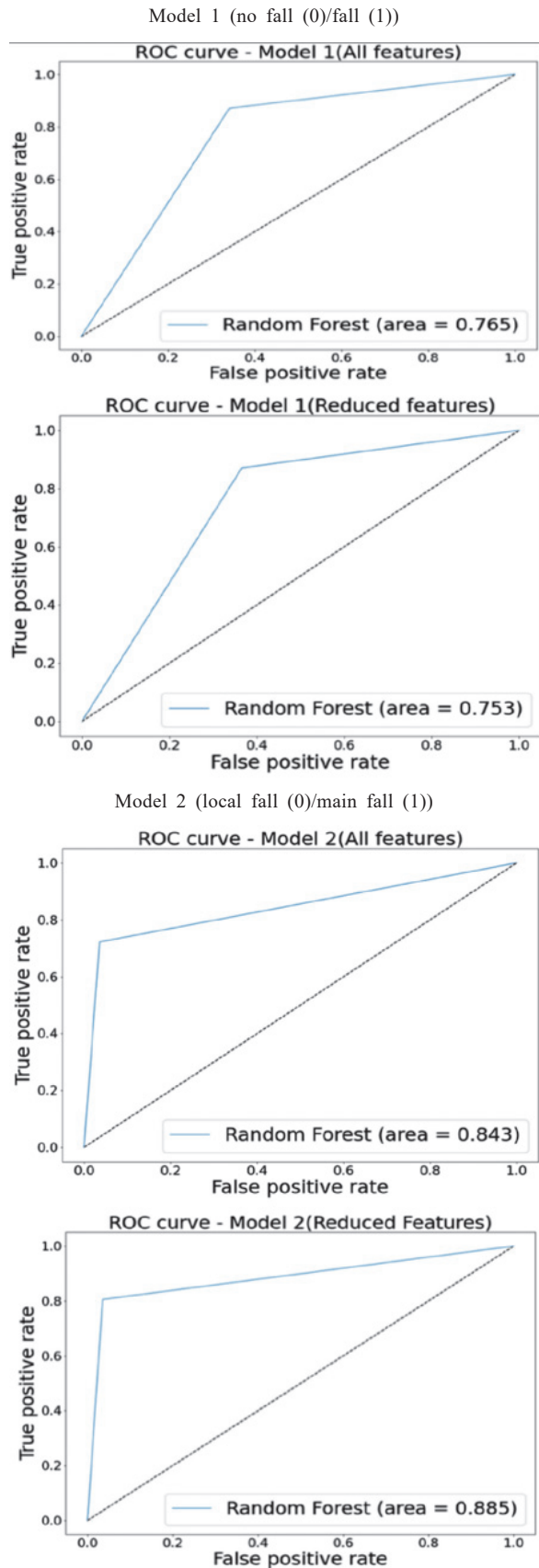


Fig.11 ROC curves of models

expressed in the paper are that of the authors and not necessarily of the organizations they belong to.

### References

- Bradley A.E (1997): The use of the area under the ROC curve in the evaluation of machine learning algorithms. *Pattern Recognition*, 1997, 30(7), 1145–1159.
- Breiman L. (2001): Random Forests. Statistics Department University of California Berkeley, CA 94720, Jan,1–33.
- Chase F., Mark C and Heasley K. (2002): Deep cover pillar extraction in the U.S. Coalfields. In: *Proceedings of the 21st International Conference on Ground Control in Mining*. Morgantown, West Virginia University, USA; 2002, 69-80.
- Chen R.C., Dewi C., Huang S.W. and Caraka, R.E.(2020): Selecting critical features for data classification based on machine learning methods. *J. of Big Data*, 2020, 7:52,1–26. <https://doi.org/10.1186/s40537-020-00327-4>
- DGMS(1993) Cir. (Tech.) Sapicom 3/1993 & 6/1993.
- Dixit M and Mishra K. (2010): A unique experience of on shortwall mining in Indian coal mining industry. In: Bose LK, Bhattacharya BC, Ghatak GP, Editors. *Proceedings of the Third Asian Mining Congress*. Kolkata : MGMI; 2010, 25–37.
- Duzgun H.S.B and Einstein H.H. (2004): Assessment and management of roof fall risks in underground coal mines. *Safety Science* (2004),42,23–41. [https://doi.org/10.1016/S0925-7535\(02\)00067-X](https://doi.org/10.1016/S0925-7535(02)00067-X)
- Ghasemi E., Ataei M., Shahriar K., Sereshki F and Esmail S. (2012): Assessment of roof fall risk during retreat mining in room and pillar coal mines. *International Journal of Rock Mechanics and Mining Sciences*, 54, 80–89. <https://doi.org/10.1016/j.ijrmms.2012.05.025>
- Goutte C and Gaussier E (2005): A Probabilistic Interpretation of Precision, Recall and F-score, with Implication for Evaluation. *Lect Notes in Comput Sci*, 2005, 3408 (April), 345–359.
- Gupta R.N and Prajapati R.B. (1997): Improvement of roof control by laterally confined fully grouted bolts. In: *Proceedings of the 27th International Conference of Safety in Mines Research Institute*, New Delhi., 2 (February, 1997), pp 729-741.
- Harshitha P., Dixith H.S., Krithi, Rajeeva N and Shashikala (2020): Coal Mine Disaster Prediction. *Int. Journal of Engineering Research & Technology (IJERT)*, 2020, ISSN: 2278-0181, 9(07), 1447–1451.
- Jackins V., Vimal S., Kaliappan M and Lee, M. (2021): AI based smart prediction of clinical disease using random forest classifier and Naive Bayes. *The Journal of Supercomputing*, 2021, 77(5), 5198–5219. <https://doi.org/10.1007/s11227-020-03481-x>

(Continued on page 74)